LA-UR- 11-04499

Approved for public release; distribution is unlimited.

Title: Taylor Impact Tests and Simulations of Plastic Bonded Explosives

Author(s): B. E. Clements, D. G. Thompson, D.J. Luscher, R. DeLuca, and G.W. Brown

Intended for: Proceedings of the 2011 APS SCCM Meeting

Los Alamos NATIONAL LABORATORY EST.1943

TAYLOR IMPACT TESTS AND SIMULATIONS OF PLASTIC BONDED EXPLOSIVES

B. E. Clements, D. G. Thompson, D. J. Luscher, R. DeLuca and G. W. Brown

Los Alamos National Laboratory, Los Alamos NM 87545

Abstract. Taylor impact tests were conducted on plastic bonded explosives PBX 9501 and PBXN-9 for impact velocities between 80 and 214 m/s. High-speed photography was used to image the impact event at a rate of one frame for every 25 μs. For early times, PBXN-9 showed large-deformation mushrooming of the explosive cylinders, followed by fragmentation by an amount proportional to the impact speed, was observed at all velocities. PBX 9501 appeared to be more brittle than PBXN-9, the latter demonstrated a more viscoelastic response. The post-shot fragments were collected and particle size distributions were obtained. The constitutive model ViscoSCRAM was then used to model the Taylor experiments using the finite element code ABAQUS. Prior to the Taylor simulations, ViscoSCRAM was parameterized for the two explosives using uniaxial stress-strain data. Simulating Taylor impact tests validates the model in situations undergoing extreme damage and fragmentation.

Keywords: PBX, PBX 9501, PBXN-9, Taylor Impact, Constitutive Models, ABAQUS
PACS: 62.20.M-, 81.70.Bt, 83.50.-v

INTRODUCTION

Taylor impact tests were previously conducted on plastic bonded explosives (PBXs) to characterize the stress state of these materials as they impact smooth flat anvil surfaces at speeds on the order of 100 m/s [1]. The focus of that work was on the explosive PBXN-109. In 2003, C. Liu and R. Ellis performed Taylor tests on PBX 9501 up to speeds of 115 m/s, capturing impact images using high-speed photography [2]. The goal was to discover the threshold velocity for the initiation of the explosive. No threshold was observed. In the work presented here we have extended these tests to velocities in excess of 200 m/s . Using a high-speed camera, specimen images were obtained as they undergo substantial deformation, including fragmentation. The camera is capable of producing an image at a frequency of one per 25 μs. PBX 9501 and PBXN-9 are investigated here. Because of substantial differences observed in these experiments, compositional differences will be summarized. A description of the experiment will be given as well as the experimental findings, including gross observations, quantitative particle size distributions of the post-shot fragments, and early-time Taylor cylinder profiles. The thermo-mechanical constitutive model ViscoSCRAM is then used in conjunction with finite element simulations to make comparisons with the Taylor experiments. While no chemical reaction has been observed at these velocities, the Taylor test is a valuable tool for validating models in situations undergoing extreme damage and fragmentation.

MATERIALS

PBX 9501 and PBXN-9 are HMX-based explosives. PBX 9501 consists of 95 wt.% HMX and has an estane binder (with 2.5 wt.%

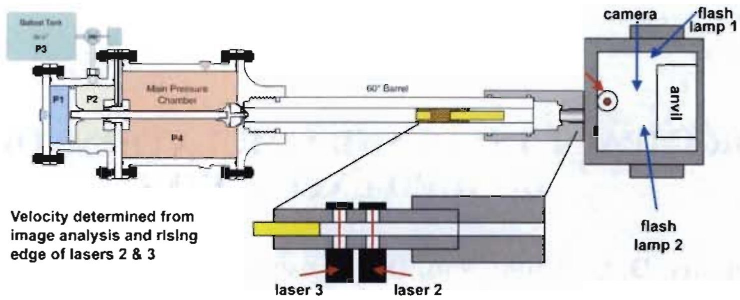

Figure 1. Schematic of the Taylor impact setup used in this study.

nitroplasticizer) , which makes up about 6.9 vol.% of the HE. The density is 1.834 g/cm^3, and a typical void content is 1.4%. PBXN-9 is 92 wt.% HMX and uses Hycar 4054, with 6% dioctyl adipate, as its binder, which makes up about 14.5 vol.% of the explosive. Note that the volume percent binder in PBXN-9 is about twice that of PBX 9501 and this will have obvious consequences in Taylor tests. The density of PBXN-9 is 1.75 g/cm^3, and a typical void content is 0.8%.

The grain size distribution is also different for the two explosives. Both PBX 9501 and PBXN-9 use coarse Class-1 HMX grains consisting of particulate sizes between 44 and 300 µm. However, PBX 9501 uses a 3:1 coarse to fine mix, whereas PBXN-9 uses a 1.2:1 coarse to fine mix. The fine grade, Class-2 HMX, in PBX 9501 has at least 75% of the particulate sizes being 44 µm or less, while the fine grade in PBXN-9 is Class-5, and has at least 98% particulates in the range of 44 µm or less. Thus, overall the explosive particulates are more homogeneous and finer in PBXN-9 [3].

Finally, uniaxial tension experiments show that PBXN-9 fails in tension at a nearly rate-insensitive strain of 0.4%. PBX 9501, is more brittle, its tensile failure strain decreases with strain rate, and at high rates a failure strain less than 0.1% can be anticipated for uniaxial conditions.

TAYLOR EXPERIMENTS

A schematic of the experimental setup is shown in Fig. 1. An oscilloscope tracks three lasers that are mounted on a composite-lined gun barrel and and in the steel box containing the anvil to trigger diagnostics and determine the projectile velocity. A Phantom 7 camera allows images to be taken at 25 µs per frame [4]. We obtained ten shots on PBX 9501 and eight on PBXN-9 for impact speeds between approximately 80 and 214 m/s. To achieve these speeds it was found necessary to omit the use of a sabot, often used in a Taylor test.

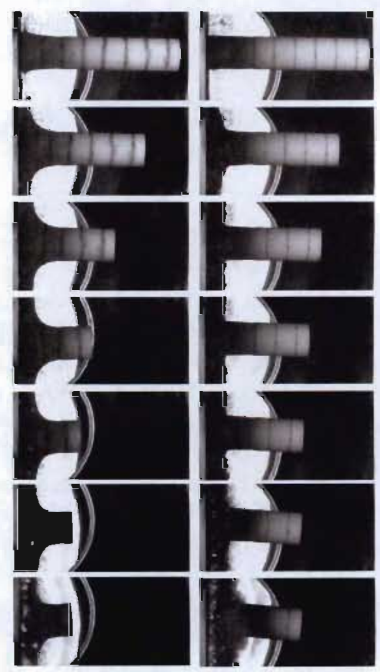

Figure 2. PBXN-9 Taylor tests at a velocity of 136.6 m/s (left), and PBX 9501 at a velocity of 132.1 m/s (right). Each frame is 100 µs in succession, with the first frame shown being at the instant of impact and the final frame being near the conclusion of the deformation.

In Fig. 2, two shots at nearly the same velocity show the quality of the information achieved in these experiments. Comparing these images show that different behavior are observed in the more viscoelastic PBXN-9 and the more brittle PBX 9501.

The first general observation is that for the same impact velocity, significantly more of PBXN-9 is consumed in the fragmentation process, than for PBX 9501. Using the intact mass of the cylinder tail as the metric, it is seen from Fig. 3, that PBXN-9 consistently has a larger mass consumed by fragmentation. Note, the initial mass of the cylinders is about 26 g, and the length and diameters are approximately 76 mm and 15 mm, respectively.

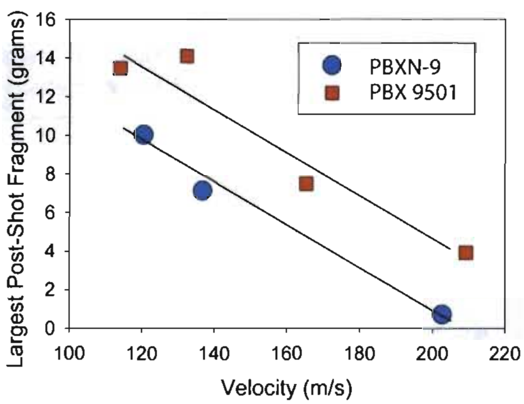

Figure 3. Largest recovered fragment (cylinder tail) for the two explosives as a function of impact velocity.

The next observation comes from the particle size distribution determined from a sieve analysis on the post-shot material. The results from the two explosives are shown in Fig. 4. PBX 9501 fragments (excluding the large tail fragment) show much less impact velocity dependence compared to PBXN-9. For a given impact speed PBXN-9 has visible concentrations of fragments of all sizes, while more of PBX 9501 has been reduced to nearly a powder. Thus more of the kinetic energy of the impacting cylinder is expended in producing fragment surface area in the case of PBX 9501 than in PBXN-9. This explains why, at the end of the deformation process, a large tail mass of the cylinder is left in the case of PBX 9501 and a smaller mass is left in the case of PBXN-9.

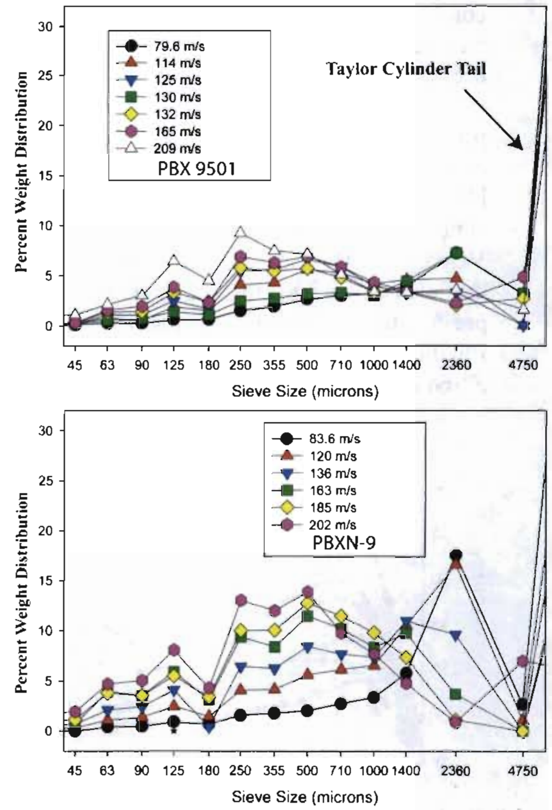

Figure 4. Sieve data for PBX 9501 (top) and PBXN-9 (bottom). Plotted is the normalized weight percent distribution as a function of the sieve size.

The final observation is that substantial mushrooming of the cylinder occurs before it fragments. The first several frames of Fig. 2 clearly show the mushrooming, especially in the case of PBXN-9.

THEORETICAL RESULTS

The quasi-static mechanical properties of PBX 9501 (Fig. 5 shows a representative plot) and PBXN-9 have been characterized in both tension and compression. In addition, LANL researchers [3] have used the Split Hopkinson Pressure Bar (SHPB) apparatus to measure the stress-strain curves at higher strain rates. This data is used to calibrate the ViscoSCRAM explosives constitutive model. The details of the model can be found elsewhere [5]. Together with ViscoSCRAM's shear crack-growth model, a simple tensile failure condition that acts at the finite-element (FE) level has been added. The FE code ABAQUS [6] is used. The tensile failure condition states that, when an element is in hydrostatic tension, and the principal tensile strain exceeds a certain value, the element will permanently cease to support a load [6]. Using this technique, fragmentation was simulated. At early times (see Fig 6) ViscoSCRAM performed well, but at later times, the element death technique gave poor results presumably attributable to the lack of fragment-fragment interactions. This work is to be viewed as a first step in modeling Taylor experiments.

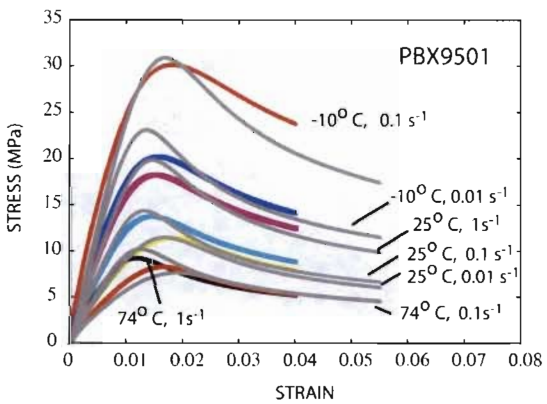

Figure 5. Low-rate uniaxial compression experimental and ViscoSCRAM model fits to PBX 9501 stress-strain curves. The theory curves are the longer ones.

CONCLUSIONS

Quantitative information on explosives undergoing large deformation may be obtained by Taylor experimentation. This information allows constitutive models like ViscoSCRAM to be tested in regimes not easily tested by other methods, especially in situations undergoing extreme damage and fragmentation.

ACKNOWLEDGEMENTS

The authors appreciate funding by the Joint DoD/DOE Munitions Technology Development Program and discussions with P. Rae, C. Cady and C. Liu. Special thanks go to Jose Archuleta (LANL) for obtaining the sieve data and LANL summer student Joe Koby, for extracting experimental cylinder profiles.

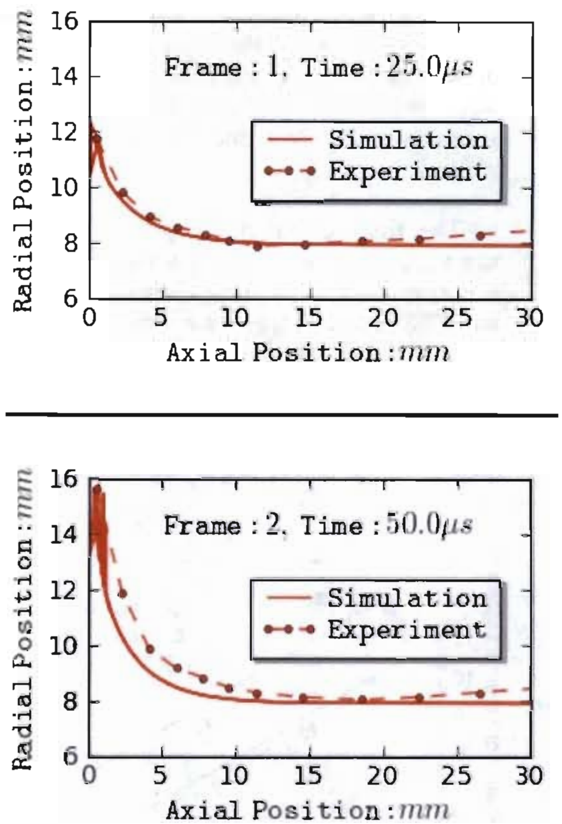

Figure 6. PBXN-9 136 m/s experiment and simulated cylinder profiles at 25 and 50 μs. At 50 μs, the jagged simulation profile between 14 and 16 mm occurs due to fragmentation. A critical tensile strain of unity was used.

REFERENCES

1. Christopher, F. R., Foster, J. C., Wilson, L. L., and Gilland, H. L., *Proceedings of the 11th International Detonation Symposium*, (1998) pp. 286.
2. Liu, C. and Ellis, R., (LANL, unpublished).
3. Gray, G. T. III, Idar, D. J., Blumenthal, W. R., Cady, C. M., Peterson, P. D., *Proceedings of the 11th International Detonation Symposium*, (1998) pp. 76.
4. PHANTOM cameras: product of ViSiON Research, an AMETEK Co.; http://www.visionresearch.com/.
5. Hackett, R. M., and Bennett, J. G., *International Journal for Numerical Methods in Engineering* **49**, 1191–1209, (2000).
6. Abaqus FEA, a SIMULIA Product, http://www.simulia.com/.